行政院國家科學委員會補助專題研究計畫成果報告

※※※※※※※※※※※※※※※※※※※※※※※※※
※　　　　　　　　　　　　　　　　　　　　　　　※
※　　多參考站架構下建基於 GPS 之軌跡判定　　　※
※　　　　　　　　　　　　　　　　　　　　　　　※
※※※※※※※※※※※※※※※※※※※※※※※※※

計畫類別：☑ 個別型計畫　　□ 整合型計畫

計畫編號：NSC 89-2213-E-002-153

執行期間：89 年 8 月 1 日至 90 年 7 月 31 日

計畫主持人：張帆人

共同主持人：

本成果報告包括以下應繳交之附件：

- □ 赴國外出差或研習心得報告一份
- □ 赴大陸地區出差或研習心得報告一份
- ☑ 出席國際學術會議心得報告及發表之論文各一份
- □ 國際合作研究計畫國外研究報告書一份

執行單位：台灣大學電機系

中　華　民　國　90 年　10 月　30 日

多參考站架構下建基於 GPS 之軌跡判定

計畫編號：NSC 89-2213-E-002-153

執行期限：89 年 8 月 1 日至 90 年 7 月 31 日

主持人：　張帆人　台灣大學電機系教授

一、中文摘要 (關鍵詞：GPS、卡門濾波器、平滑器、衛星導航)

我們利用 PVA (Position Velocity Acceleration) 模型來模擬載具運動情形，並利用差分式衛星定位演算法作為量測方程式，代入卡門濾波器 (Kalman Filter) 之遞迴程序中。然後，我們進一步結合順向濾波器與逆向濾波器成為平滑器 (Smoother)。除了平滑處理外，我們還利用最小化均方差法，結合多個參考站的定位平滑結果，以減少在某段時間內的定位誤差影響。我們建構整個系統的軟體與硬體，並在校園中驗証所推導的理論。

Abstract (Keywords: GPS, Kalman Filter, Smoother, Satellite Navigation)

By using PVA (Position Velocity Acceleration) model, the dynamic vehicle can be simulated. Differential GPS algorithms play the roles of the measurement equations in the recursive processes of Kalman Filter. Besides this, we combine the forward filter and backward filter to be the smoother in order to achieve the higher precision. Then we use MMSE (Minimum Mean Square Error) to integrate different smoothing results from different reference stations for reducing positioning error. Finally we construct the hardware and the software of the system. Also, we check the smoothed results from multi reference stations to confirm our algorithm.

二、緣由與目的

隨著科技的進步，GPS 的應用也漸趨於廣泛與務實。如何提升 GPS 的定位精度與適應性，則成當務之急。如果能妥善利用多個參考站來定位，不但有可能提高定位精度，也可以預防應為某個參考站突然失效而無法定位的情形發生。

三、研究方法

以下，即為三座參考站架構下軌跡判定的示意圖：

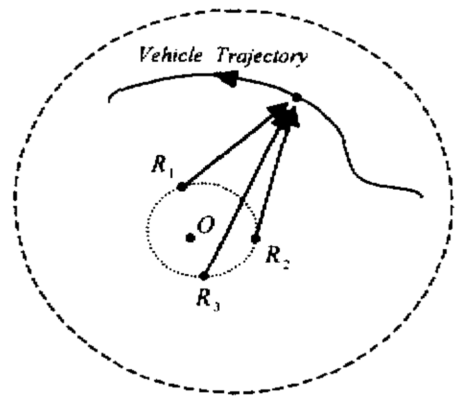

R_i：第 i 座參考站

圖一 三座參考站架構之軌跡判定

在多個參考站的架構下，可以利用各個不同的參考站來得到相對定位，形成多個不同軌跡。若能將這些軌跡適當整合，所獲得的那條軌跡將最接近實際的狀況，依照這種觀念，我們提出整合這些軌跡的方法是平滑器整合法。接下來再利用最小化均方誤差（Minimum Mean Square Error, MMSE）的方法，結合這些平滑後的軌跡，得到最後的定位結果。

因為軌跡是經相對定位後得到的結果，所以，每一座參考站本身的座標事前就要以測量級的 GPS 接收機(Ashtech Z-12、Z-survey 等)，將其精準定位。如此，相對定位的軌跡才能呈現在同一座標之上。(我們利用內政部衛星測量中心提供的多個一等或二等三角點，以測量級接收機引到預定的參考站)。

現考慮第一個參考站（R1）的狀況，如圖二所示：

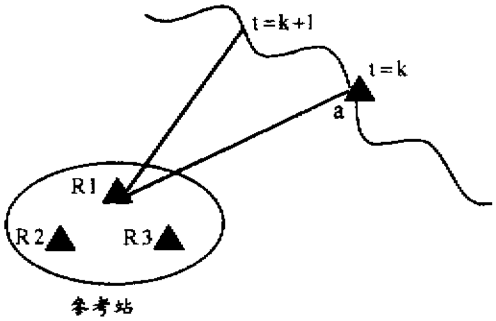

圖二 工作模型

則我們可從此工作模型推出載具的運動過程與平滑器演算法。

1. 動態方程式建立

從圖二的工作模型，可知對單一參考站，載具從 $t=k$ 秒至 $t=k+1$ 秒的移動情形，可以寫成以下的數學式：

$$X_{k+1}=\Phi_k X_k+w_k \qquad E\left[w_k w_k^T\right]=Q_k \qquad w_k \text{為程序誤差}$$

$$Z_k=H_k X_k+v_k \qquad E\left[v_k v_k^T\right]=R_k \qquad v_k \text{為量測誤差}$$

$$\text{其中}X_k=\begin{bmatrix}x_1\\x_2\\x_3\\x_4\\x_5\\x_6\\x_7\\x_8\\x_9\end{bmatrix}_k=\begin{bmatrix}x_R-x_a\\y_R-y_a\\z_R-z_a\\v_x\\v_y\\v_z\\a_x\\a_y\\a_z\end{bmatrix}_k \qquad \begin{array}{l}x_1=\text{參考站i與待測物a的X座標距離}\\x_2=\text{參考站i與待測物a的Y座標距離}\\x_3=\text{參考站i與待測物a的Z座標距離}\\x_4=\text{待測物在X座標投影的移動速度}\\x_5=\text{待測物在Y座標投影的移動速度}\\x_6=\text{待測物在Z座標投影的移動速度}\\x_7=\text{待測物在X座標投影的加速度}\\x_8=\text{待測物在Y座標投影的加速度}\\x_9=\text{待測物在Z座標的投影加速度}\end{array}$$

若忽略誤差項，我們可得 X_k 的估測值 $\hat{X}_k$，與其下一個狀態的關係 $\hat{X}_{k+1}=\Phi_k\hat{X}_k$，其中

$$\Phi_k=\begin{bmatrix}1&0&0&\Delta t&0&0&\frac{1}{2}\Delta^2 t&0&0\\0&1&0&0&\Delta t&0&0&\frac{1}{2}\Delta^2 t&0\\0&0&1&0&0&\Delta t&0&0&\frac{1}{2}\Delta^2 t\\0&0&0&1&0&0&\Delta t&0&0\\0&0&0&0&1&0&0&\Delta t&0\\0&0&0&0&0&1&0&0&\Delta t\\0&0&0&0&0&0&1&0&0\\0&0&0&0&0&0&0&1&0\\0&0&0&0&0&0&0&0&1\end{bmatrix}$$

我們可由 GPS 差分定位法 $\nabla\Delta\rho=Hb$，改寫成量測方程式 $Z_k=H_kX_k$，如下示：

$$\begin{bmatrix}\nabla\Delta\rho^{ij}_{mr}\\\nabla\Delta\rho^{ik}_{mr}\\\nabla\Delta\rho^{il}_{mr}\\\vdots\end{bmatrix}_k=\begin{bmatrix}\frac{\partial\rho^i(x^m)}{\partial x}-\frac{\partial\rho^j(x^m)}{\partial x}&\frac{\partial\rho^i(y^m)}{\partial y}-\frac{\partial\rho^j(y^m)}{\partial y}&\frac{\partial\rho^i(z^m)}{\partial z}-\frac{\partial\rho^j(z^m)}{\partial z}&0_{1\times6}\\\frac{\partial\rho^i(x^m)}{\partial x}-\frac{\partial\rho^k(x^m)}{\partial x}&\frac{\partial\rho^i(y^m)}{\partial y}-\frac{\partial\rho^k(y^m)}{\partial y}&\frac{\partial\rho^i(z^m)}{\partial z}-\frac{\partial\rho^k(z^m)}{\partial z}&0_{1\times6}\\\frac{\partial\rho^i(x^m)}{\partial x}-\frac{\partial\rho^l(x^m)}{\partial x}&\frac{\partial\rho^i(y^m)}{\partial y}-\frac{\partial\rho^l(y^m)}{\partial y}&\frac{\partial\rho^i(z^m)}{\partial z}-\frac{\partial\rho^l(z^m)}{\partial z}&0_{1\times6}\\\vdots&\vdots&\vdots&\vdots\end{bmatrix}\begin{bmatrix}x^m-x^r\\y^m-y^r\\z^m-z^r\\v^x\\v^y\\v^z\\a^x\\a^y\\a^z\end{bmatrix}$$

如此即可架構出動態方程式。而我們所採用的平滑器演算法則是整合順向與逆向濾波器的結果。

2. 加入其它的參考站

現回到原來的工作模型，在有三個參考站的情形下，將每個參考站的定位結果分別經過平滑器處理，則可獲得 $\hat{X}_1(t|N)$、$\hat{X}_2(t|N)$、$\hat{X}_3(t|N)$，和相對應的誤差偏方矩陣 $P_1(t|N)$、$P_2(t|N)$、$P_3(t|N)$，如此則可以經由最小均方誤差（MMSE）法，來推出其最佳估測值。

$$\hat{X}'=\hat{P}'[P_1^{-1}(t|N)\hat{X}_1(t|N)+P_2^{-1}(t|N)\hat{X}_2(t|N)+P_3^{-1}(t|N)\hat{X}_3(t|N)]$$

其中 $\hat{P}'=[P_1^{-1}(t|N)+P_2^{-1}(t|N)+P_3^{-1}(t|N)]^{-1}$

如此一來，即可得到整合不同參考站的定位軌跡。

四、研究成果

1. 模擬

在實地實驗之前，我們先對平滑器和多參考站演算法作簡單的模擬，以檢驗演算法的正確性。由表一可看出經過濾波處理後，其位置皆比未經過濾波處理的量測值要好得多，尤其以平滑處理後的改善最佳。

表一 濾波與平滑結果與實際軌跡比較之誤差

處理過程／誤差	未經處理	經順向濾波器處理	經逆向濾波器處理	經平滑器處理
取樣平均值	0.8171	0.6303	0.6065	0.3094
取樣標準差	0.6236	0.4877	0.5097	0.2184

我們亦將參考站之軌跡判斷與實際軌跡比較後的誤差列於表二。由此可以看出，越多參考站的加入，其整合後的結果會越理想。

表二 多參考站與實際軌跡比較之誤差

處理過程／誤差	第一參考站平滑軌跡	第二參考站平滑軌跡	整合第一與第二站	第三參考站平滑軌跡	整合第一、二、三站
平均值	0.3094	0.3063	0.1584	0.3500	0.1528
標準差	0.2184	0.2488	0.1451	0.2414	0.0983

2. 實驗

載波相位平滑器之實驗結果示於圖三。我們發現平滑後的軌跡將在順向濾波器與逆

向濾波器的曲線之間，且順向濾波和逆向濾波的結果也比單用最小平方法直接解的方法要好得多。

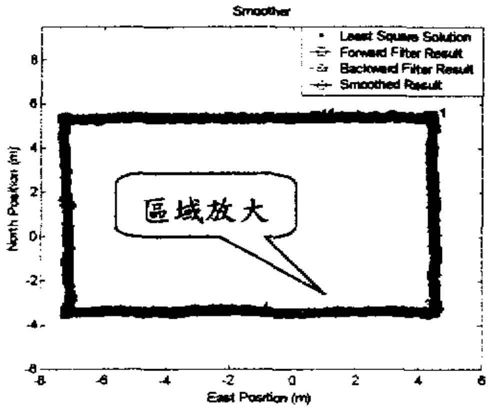

圖三 (a) 載波相位平滑器演算法的平面結果

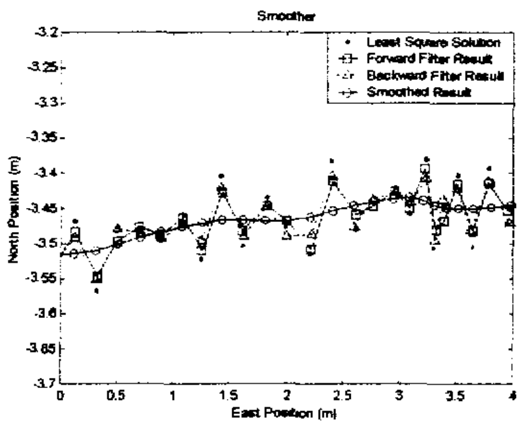

圖三(b) 載波相位平滑器演算法的平面結果

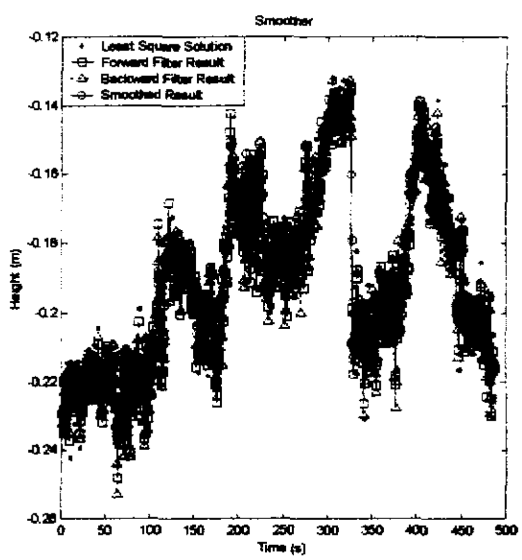

圖三(c) 載波相位與平滑器演算法的高程結果

在台大應力所樓頂上，我們設立了兩個參考站 (編號 3, 4) 並以推車作為移動站。利用載波相位實驗結果如圖四所示。

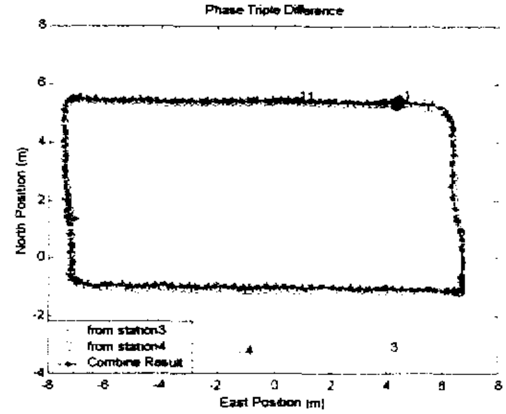

圖四 雙參考站利用載波相位平滑器之結果

五、討論與結論

在本研究中，我們建構出平滑器和多參考站演算法，以提高定位精度。其主要的原理在於如何『有效地平均』多個不同參考站的定位資料。在處理的過程中，我們放棄以往單純直接將多個不同軌跡等權平均，而利用誤差偏方矩陣來針對各個不同的定位軌跡取不同的權重，增加應用上的彈性。針對在運動中的物體，我們引入平滑器演算法，利用卡門濾波器的預估原理，來決定經過平滑處理後的最佳估測值及其誤差偏方矩陣。

六、參考文獻

[1] Elliott D. Kaplan, "*Understanding GPS : Principles and Applications*", Artech House Inc., 1996.

[2] Yaakov Bar-Shalom and Thomas E. Fortmann, "*Tracking and Data Association*", Academic Press, Inc., 1988.

[3] A. Gelb, "Applied Optimal Estimator", MIT Press, 1974.

出席國際學術會議心得報告及發表之論文

會議時間及地點　2000.9.19 ~ 2000.9.22
Marbella, Spain

會議名稱　(中文)　IASTED 國際會議　訊號處理與通訊 SPC'2000
(英文)　IASTED International Conference Signal Processing and Communication, SPC'2000

發表論文題目　(中文)　GLONASS 載波相位量測之週波脫落偵測
(英文)　Cycle-slip Detection in GLONASS Carrier Phase Measurements

報告內容

一、參加會議經過

IASTED 是國際學術組織，總部位於加拿大的 Calgary。每年在世界各地召開數十場次的學術研討會，主題以控制、通訊、電力、計算機為主。本次會議是訊號處理和通訊，因其和我多年研究衛星導航接收機部分密切相關，故投稿參加。

二、與會心得

會場位於歐洲，所以有較多的機會接觸到美國以外的學者、專家，互相切磋觀摩。此外，西歐在人文藝術上的傲人成就，也值得我們景仰。

三、建議

研討會方式的學術交流兼顧廣度和深度，對於激勵國內學者之研究興趣和熱誠士氣都有正面的功能。即使政府財政困難，現有的鼓勵措施仍應勉力而為，千萬不要打折。

四、攜回資料名稱及內容

攜回本次研討會之論文集一冊。

五、發表論文如後頁

Proceedings of the IASTED International Conference
SIGNAL PROCESSING AND COMMUNICATIONS
September 19-22, 2000, Marbella, Spain

CYCLE-SLIP DETECTION IN GLONASS CARRIER-PHASE MEASUREMENTS

Y. T. CHIANG*, F. R. CHANG* and L. S. WANG**
*Dept. of Electrical Engineering, National Taiwan University
** Inst. of Applied Mechanics, National Taiwan University
Taipei, Taiwan, Republic of China

KEYWORDS: GLONASS, Cycle-Slip, Fault Detection, Clock Error Prediction.

ABSTRACT

The availability of GLONASS system is sensitive to visible satellites. In light of the apparent lack of financial support to maintain the system through new launches, the GLONASS system users must make the best possible use of the resources. In this paper, we present a method for detecting cycle-slip that can reduce the redundant carrier-phase measurements. By modeling the behavior of the local oscillator, receiver's clock error can be predicted. The predictable clock error will be used to monitor cycle-slip occurrence. In conventional positioning algorithms, there are 4 unknown variables, x, y, z and receiver clock error. Hence, at least 4 GLONASS satellite measurements are needed for position fixing. At least 5 and 6 visible satellite measurements are needed for detection and identification of single fault satellite, respectively. By the help of predicted receiver clock error, the unknown variables become 3. In our algorithms, the needed numbers of visible satellites for fault detection and identification are 4 and 5, respectively. The experimental results are provided to verify our methods.

INTRODUCTION

The global navigation satellite system (GLONASS) is a space-based, worldwide and around the clock navigation system. The satellite constellation and the signal structure are similarly to those of global positioning system (GPS). Their major differences are the reference frame, the system time and the frequencies of the satellite signals.

Conceptually, GLONASS operates on the principle of trilateration. The accuracy of the positioning results heavily depends on the precision of the measured distances from the user to visible satellites. There are two observables being used to calculate the distances: code-phase and carrier-phase. The former one represents the radio signal travelling length from the satellite to the receiver. The code-phase can provide the range data with a coarse resolution (several meters). The later one is caused by the Doppler shift, which is proportional to the relative velocity between the satellite and the receiver. The carrier-phase can provide the range rate data with a fine resolution (one-half centimeter). In some algorithms, such as CSC (Carrier Smooth Code), these two data are integrated to obtain a balance solution. In other algorithms, such as real time kinematics (RTK), the carrier-phase data are used alone for positioning once the ambiguity values been resolved by search method. If the code-phase signal is lose track, the receiver will disconnect the associated information. However, even if the carrier-phase signal is lose track, the receiver still provides the abnormal data without any warning. Hence, for detecting and identifying the abnormal carrier-phase data are important.

GLONASS CARRIER-PHASE OBSERVABLES

The GLONASS carrier-phase observables count the beat phase, i.e., the difference between the L_1-band carrier wave from a satellite and the reference signal generated by the receiver. It can be modeled as

$$\lambda^j \phi_A^j = \rho_A^j + c(dt^j - dT_A) + \lambda^j N_A^j - d_{ion}^j + d_{trop}^j + \varepsilon_A^j$$

(1)

where ϕ_A^j is the carrier-phase measurements of the receiver A from the j-th GLONASS satellite; ρ_A^j is the true distance between the receiver A and the j-th satellite; c

is the speed of light; N_A^j denotes the initial phase integer ambiguity; d_{ion}^j, d_{trop}^j, and ε_A^j are the ionospheric delay, the tropospheric delay and the unmodeled errors, respectively; dt^j is the clock error of the j-th satellite, and dT_A denotes the clock error of the receiver A. $\lambda^j = c/f^j$, f^j is the frequency of satellite j. Because the GLONASS is employed the technique of frequency division multiple access (FDMA) to distinguish the signals from the different satellites, each satellite uses common PRN code but different carrier frequencies. The frequency offset between satellites in the L_1 band is 562.5 kHz

$$f^j = 1602\,\text{MHz} + j \times 0.5625\,\text{MHz},$$

where j is the channel number.

If the distance from the mobile receiver A and the reference station B is short, the effects of the propagation delay will be nearly same. Then, by forming the phase difference between the mobile user and the reference station, the common error factor dt^j, d_{ion}^j and d_{trop}^j in (1) can be eliminated. Furthermore, forming the phase difference from one epoch to the next, the initial phase integer ambiguity can be eliminated. One advantageous model, namely receiver-time double difference, is to perform the change from one epoch to the next and to obtain the difference between receivers for the same satellite. The equation in receiver-time double difference is expressed as

$$\lambda^j \delta\Delta\phi_{AB}^j = \delta\Delta\rho_{AB}^j - c\delta\Delta dT_{AB} + \delta\Delta\varepsilon_{AB}^j, \tag{2}$$

where the convention $\delta\Delta *_{AB}^j = (*_B^j - *_A^j)_{epoch2} - (*_B^j - *_A^j)_{epoch1}$ is used, and the asterisk may be replaced by ϕ, ρ, cdT and ε.

With n satellites ($n \geq 4$) being observed at the same time, the matrix form (2) is written as

$$\delta\Delta\phi_{AB} = H \cdot u + \delta\Delta\varepsilon_{AB}, \tag{3}$$

where $\delta\Delta\vec{\phi}_{AB}$ is an n-tuple vector; the j-th element is $\lambda^j \delta\Delta\phi_{AB}^j$. $H(n \times 4, n \geq 4)$ is the observation matrix, the j-th row of H is $[e_A^j \ \ 1]$, e_A^j denotes the line-of-sight (unit) vector from user A to satellite j. u is a 4-tuple state vector $u = [\delta x \ \delta y \ \delta z \ c\delta\Delta dT_{AB}]^T$, denoting the displacement and the difference in clock error between receiver A and B. The least square solution of (3) is

$$\hat{u} = (H^T H)^{-1} H^T \cdot \delta\Delta\Phi_{AB}, \tag{4}$$

where $\hat{u}$ is the estimation of the true state u.

THE PREDICTION OF CLOCK ERROR

some receivers employ high precision, oven-controlled, quartz crystal oscillators. These oscillators are small, light-weight, consume little power and are relatively inexpensive. They have sufficient short-term stability to add negligible noise to code tracking loops and their long-term drift can be measured and modeled using the GLONASS signals themselves.

In (1) the clock error dT_A is caused by the stability of receiver local frequency. This error can be eliminated by double difference-method between satellites and receivers. However, by exploiting the short-term stability of receiver quartz oscillator, the clock error can be modeled and predicted. The used model is [1]:

$$dT_A(t) = a_A + b_A \times t + Dr_A \times \frac{t^2}{2} + \varphi_A(t), \tag{5}$$

where $dT_A(t)$ is the receiver A's clock error that is related to its nominal standard clock; a_A and b_A are clock bias and clock drift, Dr_A denotes the clock drift rate, and $\varphi_A(t)$ is the random part.

Substitutes (5) into (2), the difference of receiver clock error becomes

$$\begin{aligned}\delta\Delta dT_{AB} &= \Delta dT_{AB}(t_{epoch2}) - \Delta dT_{AB}(t_{epoch1}) \\ &= a_{AB} + b_{AB}\tau + \frac{1}{2} Dr_{AB}\tau^2 + \varepsilon_\varphi\end{aligned}$$

(6)

where $a_{AB} (= a_B - a_A)$ is the difference of clock bias, $b_{AB} (= b_B - b_A)$ and $Dr_{AB} (= Dr_B - Dr_A)$ are the difference of clock drift and drift rate between the receiver A and B, and τ denotes the fixed time interval from one epoch to the next. Figure 1 shows the clock behavior of reference receiver and user receiver. Because the nominal clock of two receivers is unique, the difference of clock error $\delta\Delta dT_{AB}$ is equal to the difference of the two receiver's clock.

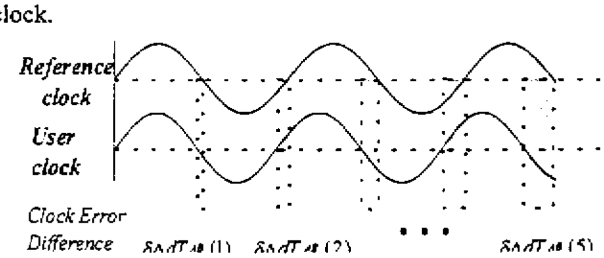

FIG. 1 The Difference of Clock Error Between Reference Receiver and User Receiver

Assume that we had observed N ($N \geq 3$) continuous GLONASS measurements and computed N $\delta\Delta dT_{AB}$ s, (6) can than be written in the form:

$$\delta\Delta dT_{AB}(n) = a_{AB} + b_{AB}\tau \cdot n + \frac{1}{2}Dr_{AB}\tau^2 \cdot n^2 + \varepsilon_\varphi(n), \qquad (7)$$

for $n = 1, 2, \cdots, N$. Let's define the matrices:

$$\overline{X} = \begin{bmatrix} \delta\Delta dT_{AB}(1) \\ \delta\Delta dT_{AB}(2) \\ \vdots \\ \delta\Delta dT_{AB}(N) \end{bmatrix}, \qquad (8a)$$

$$\overline{N} = \begin{bmatrix} 1 & 1 & 1 \\ 1 & 2 & 4 \\ \vdots & \vdots & \vdots \\ 1 & N & N^2 \end{bmatrix}, \qquad (8b)$$

$$\overline{T} = \begin{bmatrix} 1 & 0 & 0 \\ 0 & \tau & 0 \\ 0 & 0 & \tau^2 \end{bmatrix} \text{ and} \qquad (8c)$$

$$\overline{B} = \begin{bmatrix} a_{AB} \\ b_{AB} \\ \frac{1}{2}Dr_{AB} \end{bmatrix}. \qquad (8d)$$

From these definitions, equation (6) can be rewritten in the matrix form:

$$\overline{X} = \overline{N}\,\overline{T}\,\overline{B} + \overline{\varepsilon}_\varphi \qquad (9)$$

and the coefficients, $\overline{B}$, which minimize the squared errors are given by

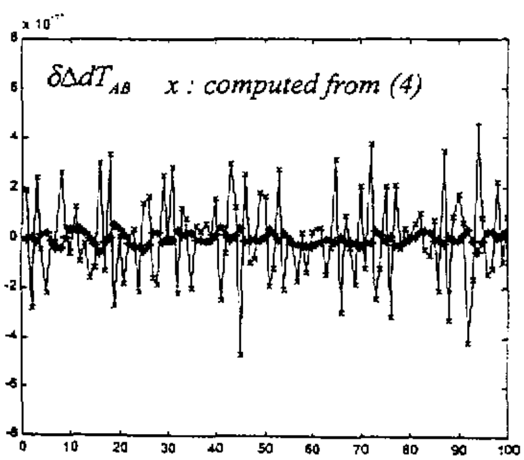

FIG. 2 Clock Errors Between Computed and Predicted

$$\hat{\overline{B}} = \begin{bmatrix} \hat{a}_{AB} \\ \hat{b}_{AB} \\ \frac{1}{2}\hat{D}r_{AB} \end{bmatrix} = \overline{T}^{-1}(\overline{N}^T\overline{N})^{-1}\overline{N}^T\overline{X} \qquad (10)$$

If $\hat{\overline{B}}$ is obtained, it is easy to predict the difference of clock error between receiver A and B at epoch N+1. The predicted equation is given by

$$\delta\Delta d\hat{T}_{AB}(N+1) = \hat{a}_{AB} + \hat{b}_{AB}\tau \cdot (N+1) + \frac{1}{2}\hat{D}r_{AB}\tau^2 \cdot (N+1)^2. \quad (11)$$

Figure 2 shows the clock errors of computed value and predicted value that they are observed from four visible satellites without cycle-slip.

DETECTION OF CYCLE-SLIP

Suppose

$$A = (H^T H)^{-1} = \begin{bmatrix} A_{11} & A_{12} & A_{13} & A_{14} \\ A_{21} & A_{22} & A_{23} & A_{24} \\ A_{31} & A_{32} & A_{33} & A_{34} \\ A_{41} & A_{42} & A_{43} & A_{44} \end{bmatrix}, \quad (12a)$$

where H is the observation matrix, then the time dilution of precision (*TDOP*) is

$$TDOP = \sqrt{A_{44}}. \qquad (12b)$$

As shown in (4), receivers can update or reset their internal clocks to standard time by solving the clock error from the pseudo-range or carrier-phase measurements. The clock error depends on oscillator stability and the variance σ_T^2 is related to carrier phase residual error variance. If the computation of clock error was accomplished through four or more satellites, than

$$\sigma_T = TDOP \times \sigma_\rho, \qquad (14)$$

where σ_ρ^2 is the measured carrier-phase residual error variance. If the measurement was accomplished by tracking a single satellite from an exactly known location, then $\sigma_T = \sigma_\rho$. In general, the measurements contain all visible satellite's signals.

To detect the cycle-slip in carrier-phase measurements, by applied relationship in (14), we can make the decision strategy for the detection threshold to monitor the difference of clock error. Figure 3 and figure 4 show the

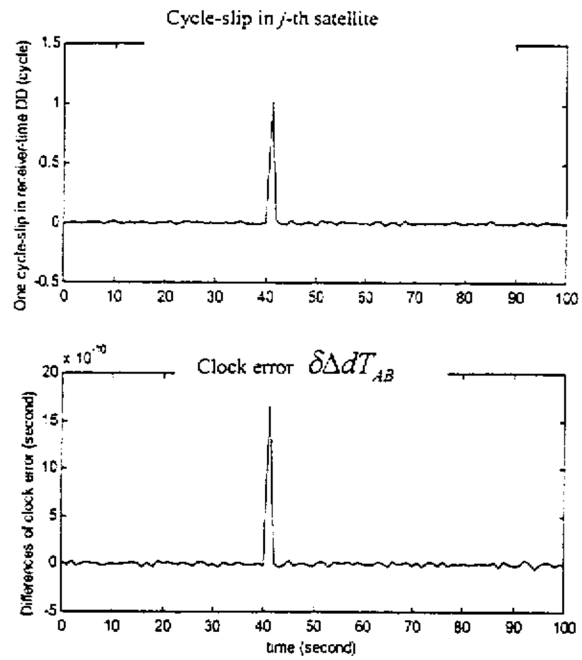

FIG. 3 Static Test of One Cycle-Slip Occurrence

occurrences of one cycle-slip under static and dynamic cases. In the two figures, $\delta\Delta\phi^{j}_{AB}$ is indicated the time-receiver double differences of carrier-phase observables on abnormal satellite, and $\delta\Delta dT_{AB}$ is the estimation of the

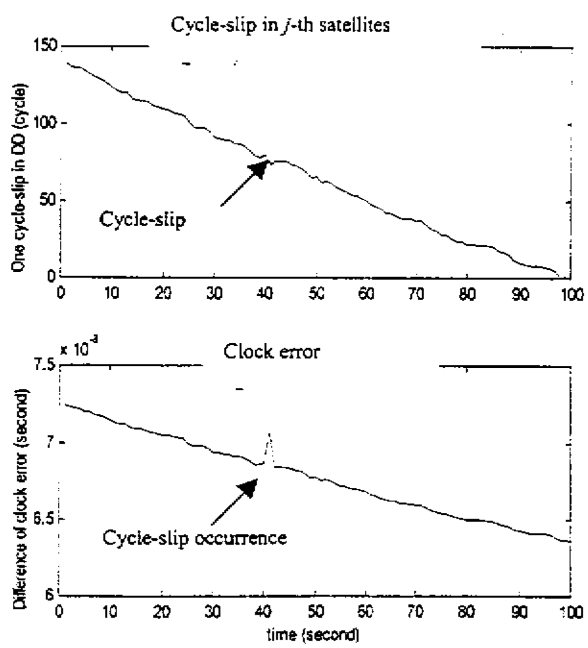

FIG. 4 Dynamic Test of One Cycle-Slip Occurrence

differences of receiver clock errors. In static test, the obvious abrupt changes in both $\delta\Delta\phi^{j}_{AB}$ and $\delta\Delta dT_{AB}$ are observed. In dynamic test, the abrupt changes of $\delta\Delta dT_{AB}$ is also obviously indicated. Because it is difficult to distinguish the phase changes between cycle-slip and receiver motion, the abrupt changes of $\delta\Delta\phi^{j}_{AB}$ can not be observed clearly. The difference of receiver clock errors $\delta\Delta dT_{AB}$ is a significant signal to make the decision for cycle-slip detection

FAULT IDENTIFICATION–PARITY SPACE METHOD

As show in (3), there are 4 unknowns, $\delta x, \delta y, \delta z$ and $c\delta\Delta dT_{AB}$ to be determined from the measurements. In conventional positioning algorithms, it needs at least four visible satellites. For detecting any single fault satellites, measurements from 5 satellites is the minimal requirement. For identifying which satellite is abnormal, measurements from 6 satellites is the minimal requirement. In this paper, $\delta\Delta dT_{AB}$ can be predicted as expressed in (11). Hence, the number of unknowns decreases to 3, i.e. $\delta x, \delta y, \delta z$. For identifying the abnormal satellite, only 5 GLONASS satellites will be enough. The parity space method can be used to identify the wrong satellite. This algorithm is described in the following.

Substituting the difference of predicted clock error that we obtained in (11) into (2), then we have

$$\Delta\Phi_{T} = G \cdot \bar{a} + e, \qquad (15)$$

where G is the first three columns of H in (3), and $\bar{a} = [\delta x \ \delta y \ \delta z]^{T}$ denotes the displacement of user receiver, $\Delta\Phi_{T} = \delta\Delta\phi^{j}_{AB} - c\delta\Delta d\hat{T}_{AB}$, and $e = \delta\Delta\varepsilon_{AB}$. The least square solution of (15) is

$$\hat{\bar{a}} = (G^{T}G)^{-1}G^{T} \cdot \Delta\Phi_{T}. \qquad (16)$$

For explaining the concept of the parity space, we assume the measurements are obtained from 5 GLONASS satellites. In other word, the dimension of G matrix in (15) is 5 by 3. Applying the Gram-Schmidt process on the columns of G, and adding 2 more orthonormal columns, an orthogonal matrix Q^{T}, with the following properties: $Q^{T}Q = QQ^{T} = I_{5}$ and $Q \cdot G$ being the upper triangular matrix with last 2 rows being zeros. Let the matrix Q be partitioned into two parts, Q_S and Q_P. Q_S is the first 3 rows of Q, Q_P is the last 2 rows of Q. The parity vector is defined as $Q_P \cdot \Delta\Phi_T$, which can be used to identify the fault satellite. The reasons will be derived in the following.

Both sides of (15) are multiplied by Q. Then the left side becomes

$$Q \cdot \Delta\Phi_T = \begin{bmatrix} Q_S \cdot \Delta\Phi_T \\ Q_P \cdot \Delta\Phi_T \end{bmatrix}. \qquad (17a)$$

The right side becomes

$$Q \cdot (G\overline{a} + e) = \begin{bmatrix} Q_S \cdot (G\overline{a} + e) \\ Q_P \cdot e \end{bmatrix}. \qquad (17b)$$

Since $Q_P G = 0$, this implies $Q_P G\overline{a} = 0$ also. Comparing the 2nd block of (17a) and (17b), we have

$$Q_P \Delta\Phi_T = Q_P \cdot e. \qquad (18)$$

The parity space are columns of Q_P. In this case, let

$$Q_P = \begin{bmatrix} p_{11} & p_{12} & p_{13} & p_{14} & p_{15} \\ p_{21} & p_{22} & p_{23} & p_{24} & p_{25} \end{bmatrix}. \qquad (19)$$

Then $[p_{1i} \quad p_{2i}]^T$, for $i = 1, \cdots, 5$, are parity space. Without loss of generality, we assume there is a big abrupt change ε_b due to a failure in satellite 3, then e can be approximated as $[0 \quad 0 \quad \varepsilon_b \quad 0 \quad 0]^T$. Substitute e and (19) into (18),

$$\begin{bmatrix} d_1 \\ d_2 \end{bmatrix} = \begin{bmatrix} p_{11} & p_{12} & p_{13} & p_{14} & p_{15} \\ p_{21} & p_{22} & p_{23} & p_{24} & p_{25} \end{bmatrix} \cdot [0 \quad 0 \quad \varepsilon_b \quad 0 \quad 0]^T = \begin{bmatrix} p_{13} \\ p_{23} \end{bmatrix} \cdot \varepsilon_b \qquad ,(20a)$$

where

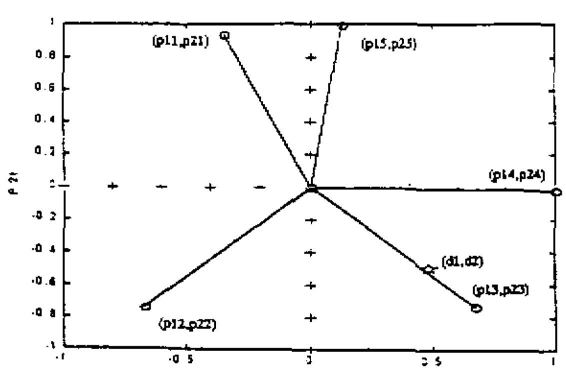

FIG. 5 Parity Space and Parity Vector Associated to the Failure of Satellite.

$$\begin{bmatrix} d_1 \\ d_2 \end{bmatrix} \equiv Q_P \cdot \Delta\Phi_T \qquad (20b)$$

is the parity vector. Figure 5 illustrates the two dimensional parity space associated with 5 satellites. The parity vector $[b_1 \quad b_2]^T$ indicates the direction of the corresponding failure in abnormal channel.

EXPERIMENTAL RESULTS

To verify our algorithms for cycle-slip detection in GLONASS carrier-phase measurements, one pair of GLONASS receivers, 3S Navigation GNSS-300 had been used. The reference station at Taipei was located at longitude 121.4138° (East), latitude 25.0215° (North), and height 50m. The tested time is set as 01:30 am~02:00 am, 22 Oct. 1999, in UTC (USNO) time. During this time interval, five GLONASS satellites (SVN 6, 7, 9, 10, 16) were observed. Among those, four satellites (SVN 6, 7, 9 and 16) were selected as the "base" satellites in the fault detection tests. The satellite SVN 10 was associated as "redundant" satellite in the fault identification tests. The data rate is 1 Hz.

Fig. 6 shows the parity space algorithm is performed. The error circle centered at the origin represents the normal condition error dispersion. The single channel fault signatures are indicated in the figure.

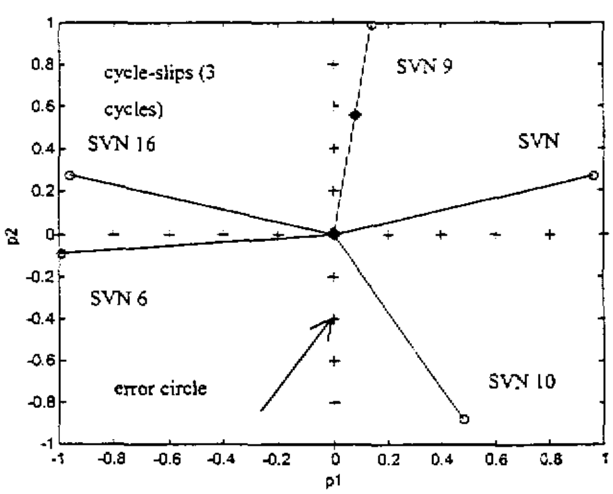

FIG. 6 Abnormal Satellite Identification

TABLE 1. Detection and Identification Statistics

Case	Sat. SVN.	Cycle-Slip (Cycles)	Numbers of Cycle-Slip Test	Fault Detection (4 satellites)	Fault Identification (5 satellites)
1	6	1	100	100%	100%
2	7	1	100	100%	100%
3	9	1	100	100%	100%
4	16	1	100	100%	100%
5	6	-1	100	100%	100%
6	7	-1	100	100%	100%
7	9	-1	100	100%	100%
8	16	-1	100	100%	100%

Table 1 shows the various situations of cycle-slip being considered. All the experiment data are real measured but the cycle-slip are artificially generated in post-processing.

CONCLUSION

This paper presents a method to detect the cycle-slip of GLONASS carrier-phase measurements by monitoring the receiver clock behavior. The method reduces the minimal requirements of redundant measurements for the cycle-slip detection and identification. Because of practical limitations, the cycle-slip detection experiment had to generate failures by artificially post-processing of previously recorded GLONASS carrier-phase measurements. As show in this paper, even one cycle-slip occurrence can be exact detected in the proposed method.

ACKNOWLEDGEMENTS

This work was supported by the National Science Council of the Republic of China under grant NSC 89-2212-E-002-081 and by 3S Navigation Corporation assistance in GNSS-300 GPS/GLONASS receivers.

REFERENCE

[1] J. A. Barnes, The Measurement of Linear Frequency Drift in Oscillators, *Proceedings of the 15th annual PTTI Meeting*, 1983

[2] E. D. Kaplan, "*Understanding GPS Principle and Applications*," Artech House, Boston 1996

[3] J. B. Neumann, M. Bates and R. S. Harvey, GLONASS Receiver Inter-Frequency Biases-Calibration Methods and Feasibility, *Proceedings of ION GPS-99*, Nashville, TN, September 14-17, 1999, pp 329-338.

[4] B. W. Parkinson and J. J. Spilker, *Global Positioning System: Theory and Applications*, Vol. I and II, AIAA, washing ton D.C., 1996

[5] B. S. Pervan, D. G. Lawrence and B. W. Parkinson, Autonomous Fault Detection and Removal Using GPS Carrier-phase, *IEEE Trans. of Aerospace and Electronic Systems*, vol. 34, No. 3, July 1998, pp. 897-906

[6] E. Rooney and A. Last, GLONASS: As Good As It Should Be?, *Proceedings of ION GPS-99*, Nashville, TN, September 14-17, 1999, pp 1363-1368.

[7] M. A. Sturga, Navigation System Integrity Monitoring Using Redundant Measurements, *Navigation, Journal of the Institute of navigation*, Vol. 35, No. 34, Winter 1988-1989, pp. 483-501